

## Optimization of Wire-bonding Process Parameters for Gold Wire and Aluminium Substrate using Response Surface Method

Megat Sufi Aniq Mohamad Rosli<sup>1</sup>, Mohd Syakirin Rusdi<sup>1,\*</sup>, Muhammad Hafiz Hassan<sup>1</sup>, Sareh Aiman Hilmi Abu Seman<sup>1</sup>, Sarudin Rohseli<sup>2</sup>, Nazmi Jamaludin<sup>2</sup> and Omar Abdul Rahman<sup>2</sup>

<sup>1</sup>School of Mechanical Engineering, Universiti Sains Malaysia, Engineering Campus, 14300, Nibong Tebal, Penang, Malaysia

<sup>2</sup>Department of Microelectronic Technologies, Advanced Technology Training Centre, 34600, Kamunting, Perak, Malaysia

### ABSTRACT

*Wire bonding is a connecting technique that uses a combination of temperature, force, ultrasonic power, and time to attach two metallic materials, a wire, and a bond pad. In electronics, gold-aluminium (Au-Al) contact wire bonds are widespread due to corrosion resistance and great conductivity of both metals. However, due to the large contact-potential difference, the intermetallic compound growth at the metal's interaction boundary has considerably worsened the advantageous properties of Au-Al intermetallic system. This intermetallic exhibit low toughness, and possibly low corrosion resistance, which would result in poor bonding quality. In this work, the materials used are 4x8 aluminium substrates and a 100-meter-long gold wire spool. This study aims to investigate the most optimised set of parameters to be used in Au-Al wire bond system, due to how problematic this system could have towards bonding quality. The experimental array was created using a response surface methodology (RSM)-based design of experiments. The effect of parameters and their significance to bonding quality in the Au-Al bond system were studied using analysis of variance (ANOVA). A correlation model was created for the wire bond strength data. The findings suggest that, within the range of parameters examined, the proposed correlation model can be utilized to predict performance measures. The optimum value of Au-Al wire bond system parameters was established at the time of bond at the first bonding site selected for 300 milliseconds (ms), wire looping height selected for 1200 micrometre ( $\mu\text{m}$ ), wire bond Y-axis length selected for 996 micrometre ( $\mu\text{m}$ ), and ultrasonic force at second bonding site selected for 300 milli Newton (mN). The outcomes of this research add to our understanding of the Au-Al wire bonding contact, in addition, to enhancing the wire bond's quality.*

**Keywords:** Wire bonding, response surface model, wire bond strength, gold-aluminium (Au-Al)

### 1. INTRODUCTION

In recent years, the quality and dependability of critical components such as light-emitting diode (LED) in medical devices, automobiles, and other applications has recently been a concern for both manufacturers and customers [1]. The most used interconnection method for semiconductor devices is wire bonding technique [2-3]. Wire bonding is an electrical wiring technique that combines temperature, force, ultrasonic power, and time to unite two metallic components, a wire, and a bond pad. [4]. High packaged interconnection reliability can be attributed in part to the advantages provided by compliant wires under conditions of temperature and bending stress [5]. In accordance with the different classification criteria, there are several kinds of wire bonding. Utilising the different capillary shapes, there are two types of bonding: ball and wedge. The three fundamental bonding procedures are thermosonic, thermocompression, and ultrasonic—can be classified based on how heating and ultrasonic work differently [6] [7].

\* Corresponding authors: syakirin@usm.my

## 2. THEORETICAL BACKGROUND

Intermetallic are chemical compounds that possess unique stoichiometry. They contain two or more metals whose atoms are arranged in a crystal lattice [8]. An example of an intermetallic compound that develops as two metals come into contact is a gold-aluminium (Au-Al) intermetallic. Due to both metals' high conductivity and resistance to corrosion, Au-Al contact wire bonds are commonly used in electronics [9-10]. However, the advantageous properties of Au and Al have been significantly impaired by the formation of intermetallic compounds at the metal-metal interaction border. These intermetallic compounds exhibit low toughness and likely limited corrosion resistance due to the significant difference in contact potential within the Au-Al system [11]. Aluminium substrate and copper wires are mainly used for low-end integrated circuit (IC) products. But, for high-end IC products, such as the military or aerospace industry, gold wire has long occupied the market with its excellent performance [12-15]. However, under high-temperature stress, the Au-Al bonding interface is prone to generate brittle compounds represented by  $Au_5Al_2$ ,  $AuAl$ ,  $Au_2Al$ , and  $Au_4Al$  [16-17], which leads to lower pull strength. Higher diffusion rates of Au and Al lead to Kirkendall effect, which increases the risk of interface rupture. The Kirkendall effect failure mechanism often triggers the effect of a ball lifting from chip metallization. The most influential factors are the parameters [18-19] including tool geometry (capillary) [19-21] and the transducer frequency [22]. In response to the problems stated above, this study uses a tabletop HB16 semi-automatic wire bonder (made by TPT Wire Bonder and manufactured in Munich, Germany) and a wire bond strength tester (made by Terra Universal and manufactured in California, United States) to determine the most optimal set of settings to be employed in Au-Al wire bond systems, to improve the quality of wire bond in Au-Al system.

## 3. MATERIAL AND METHODS

### 3.1 Designs of Experiment (DOE)

Design of experiment (DOE) was used to develop the experimental procedure. DOE is a popular technique for constructing the number of experiments needed to establish the statistically-based link between the input and output of independent variables. The central composite design (CCD), as detailed in Section 4.3, was used to create the thirty runs with perimeter values that were inserted into the HB16 – Semi-Automatic Wire Bonder for the wire bonding procedure that is presented in Table 1.

In this study, four different types of factors were examined to determine the ideal value required to establish the optimum wire bond in Au-Al systems. The four parameters are the bonding time on the first bonding site (Time 1st), the height of the wire looping (Loop Height), the bond wire's length from site one to site two (Y-axis Way), and the ultrasonic force at site two (U/S 2nd). Figure 1 below illustrates the situation for the relevant parameters.

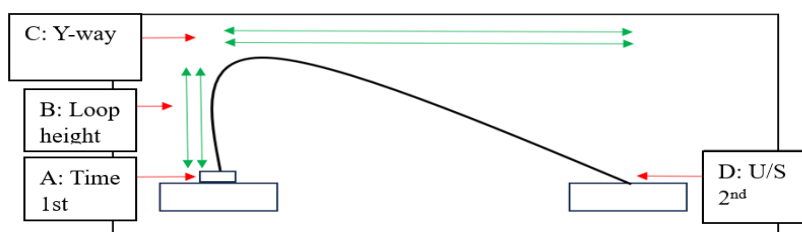


**Figure 1.** Depiction of set of parameters involved in the process.

**Table 1** Values of perimeter used for wire bonding process

<b>Run</b>	<b>A: Time 1st</b>	<b>B: Loop Height</b>	<b>C: Y-Axis Way</b>	<b>D: U/S 2<sup>nd</sup> Way</b>
1	300	1200	800	200
2	300	800	1200	300
3	200	800	800	200
4	200	1200	1200	200
5	200	800	800	300
6	250	1000	1000	300
7	250	1000	8000	250
8	250	1000	1000	250
9	250	1000	1000	250
10	300	800	800	200
11	250	1000	1000	250
12	200	1000	1000	250
13	300	1200	1200	300
14	250	1000	1000	200
15	200	800	1200	300
16	250	1000	1000	250
17	300	800	800	300
18	250	800	1000	250
19	300	1200	800	300
20	200	1200	800	200
21	200	1200	1200	300
22	300	800	1200	200
23	300	1000	1000	250
24	200	800	1200	200
25	300	1200	1200	200
26	250	1000	1000	250
27	200	1200	800	300
28	250	1000	1200	250
29	250	1000	1000	250
30	250	1200	1000	250

### 3.2 Wire Bonding Process

Figure 2 below shows the flowchart for this study wire bonding process.

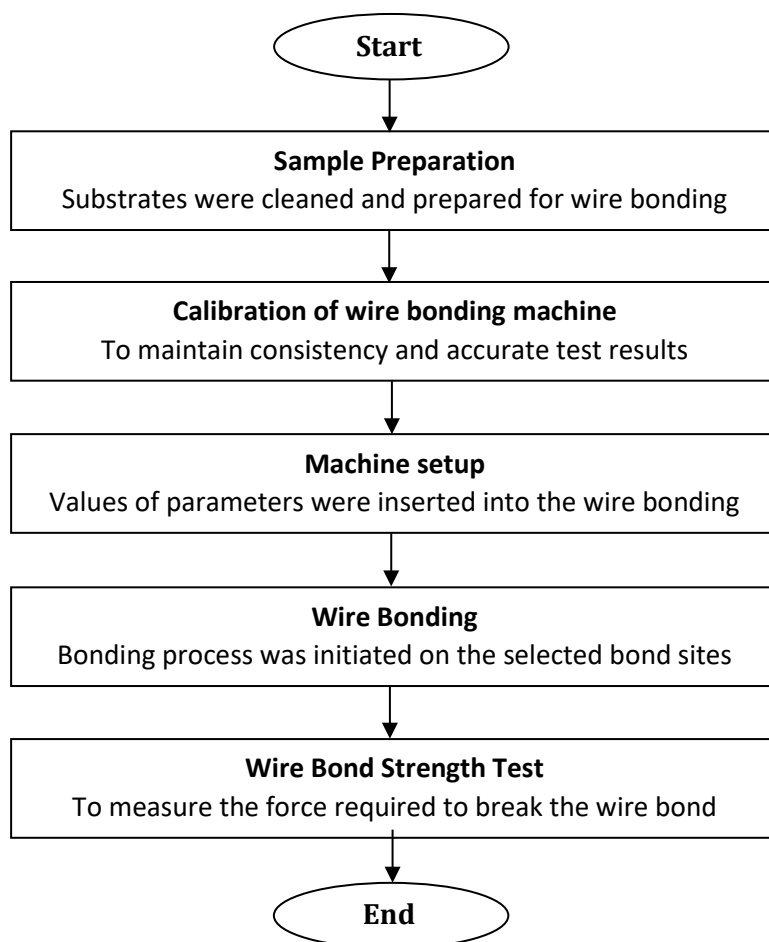


**Figure 2.** Flowchart of this study

For the procedure to be successful, the substrates are well cleaned and prepared for wire bonding. Failure of proper cleaning can lower the quality of strengths of the wire connection between bond sites on the substrates. Prior to applying pressure-sensitive process such as wire bonding, all substrate surfaces should be treated as if it was contaminated. Even newly manufactured substrates or recently cleaned surfaces will collect dust and dirt quickly and should be cleaned prior to wire bonding [23]. In this research, the substrates' surface is cleaned by using the Isopropyl Alcohol (IPA) (made by EvaChem, manufactured in Selangor, Malaysia) and cotton buds to rub it. The substrates' surface is wiped thoroughly and immediately just before the IPA evaporates. After cleaning the substrates' surface, need to make sure that the surface of the substrates is dry just before the wire bonding process begins.

A key component of instrumentation design is eliminating or reducing conditions that lead to faulty measurements. All machinery related to the wire bonding process must be calibrated to maintain its consistency of functionality and accurate test results. In this study, for the purpose of calibrating the HB16 – Semi Automatic Wire Bonder, the work stage was adjusted and the search height for bonding sites one and two were measured.

After the HB16 – Semi Automatic Wire Bonder was calibrated, the experiment was continued by inputting the desired value into the parameters workspace. Figure 3 below shows the wire bonder screen where the variety of parameter values can be altered for the wire bonding process. Such parameters are Ultrasonic (U/S), Time, Force, Loop Height, Y-way, and Heater as depicted in Figure 3. Values of parameters that were used for this study are depicted previously in Table 1.



**Figure 3.** A screen displaying parameter values that users can change.

After that, a tool called puck was used to roughly adjust the location of the first bonding site on the aluminium substrate. The puck was also used to enable the bonding head to descend onto the 'Search Height' for the first bonding site and accurately pinpointed the location of the first bonding site. Figure 4 shows the microscope used and the monitor of the HB16 – Semi-Automatic Wire Bonder to help locate the position of the bonding sites. Then, the wire bonding run was initiated, and the steps here are repeated for 29 more runs, by following the DOE stated in section 3.1.

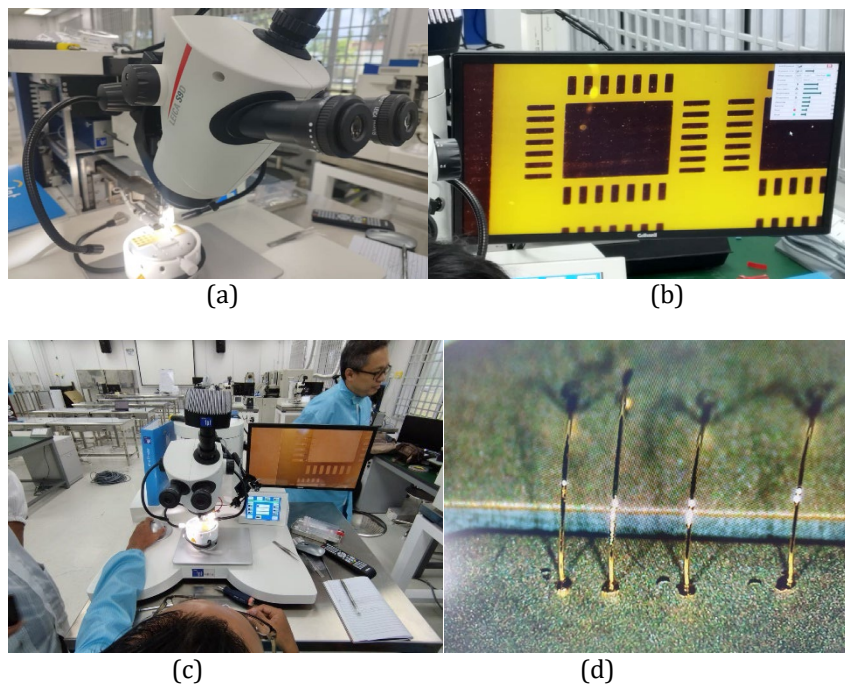


**Figure 4.** HB16-Semi Automatic Wire Bonder, (a) Microscope, (b) Monitor, (c) Front-view of the machine, (d) Resulted Au wire bond on Al substrate.

## 4. DATA COLLECTION AND ANALYSIS

### 4.1 Wire Bond Strength Test

The Al substrates with Au wire bond on it was placed on the accessory chuck, as depicted in Figure 5.

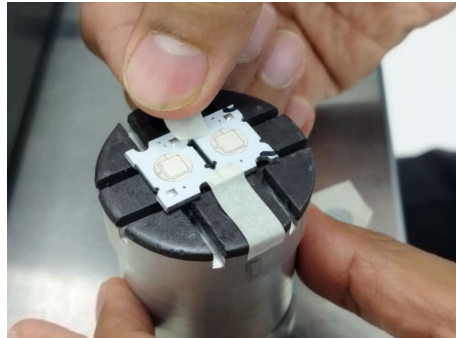


**Figure 5.** Aluminium substrates placed on the accessory chuck.

Then, by using the wire bond strength tester microscope, the actuator knob was adjusted, turned clockwise, and put into hold. This resulted in the hook being pulled in a downward motion. The hook's location was adjusted and ensured it was under the Au wire loop. Figure 6 shows the location of the tools mentioned and the schematics of the wire bond strength tester.

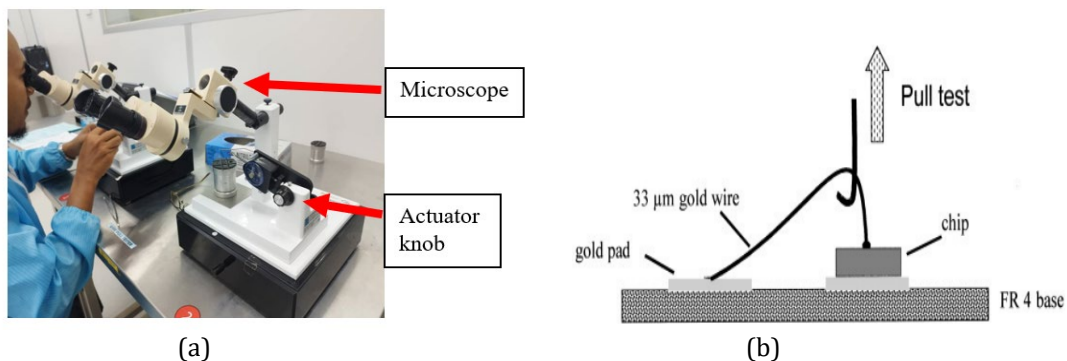


**Figure 6.** Wire bond strength tester, (a) Microscope and actuator knob on the wire bond strength tester  
(b) Schematics of wire bond strength test.

In the final step, the actuator knob was released, this would automatically turn the knob anti-clockwise, thus, pushing the hook up and breaking the Au wire loop, as seen in Figure 6 (b). The reading of the wire bond strength was recorded, and assisted by an optical microscope, the type of failure mode was identified. Data that was retrieved from performing the wire bond strength test is depicted in Table 2 below.

**Table 2** Data collected from wire bond strength test

Run	A: Time 1st	B: Loop Height	C: Y-Axis Way	D: U/S 2 <sup>nd</sup> Way	Wire Bond Strength: grams
1	300	1200	800	200	5
2	300	800	1200	300	7
3	200	800	800	200	6
4	200	1200	1200	200	5
5	200	800	800	300	5
6	250	1000	1000	300	5
7	250	1000	8000	250	6
8	250	1000	1000	250	6
9	250	1000	1000	250	5
10	300	800	800	200	5
11	250	1000	1000	250	3
12	200	1000	1000	250	6
13	300	1200	1200	300	5
14	250	1000	1000	200	4
15	200	800	1200	300	5
16	250	1000	1000	250	6
17	300	800	800	300	5
18	250	800	1000	250	5
19	300	1200	800	300	7
20	200	1200	800	200	5
21	200	1200	1200	300	4
22	300	800	1200	200	6
23	300	1000	1000	250	8
24	200	800	1200	200	5
25	300	1200	1200	200	6
26	250	1000	1000	250	4
27	200	1200	800	300	7
28	250	1000	1200	250	6
29	250	1000	1000	250	4
30	250	1200	1000	250	6

#### 4.2 Response Surface Methodology (RSM)

This research uses the help of the software, Design – Expert 13, to provide ideal experiment design and interpretation of multi-factor experiments. Factorials, fractional factorials, and composite designs are only a few of the many designs that are available in this software. Since this experiment consists of multitude of parameters such as ultrasonic power, time, and force, after entering the relevant variables into the software, Design - Expert 13 provides guidance on how to execute this experiment properly by generating a design plan. This optimisation study

looked at the interaction between the input variables. The most popular of all second-order designs, the central composite design (CCD), was used in the RSM's design. The CCD consists of a full factorial design ( $2^k$ ), where  $k$  is the number of factors, and  $2k$  of axial, star, and centre points [24]. The factors are distributed across three levels, ranging from -1 to +1. Table 3 lists the parameters that were selected for this investigation and their corresponding degrees of coding.

**Table 3** Experimental factors with coded level (Note: A=Time 1<sup>st</sup>, B= Loop height, C= Y-way, D= U/S 2<sup>nd</sup>)

Input Variables	-1 (Lower Level)	Coded Level 0	+1 (Higher Level)
A: Time 1st	200	250	300
B: Loop Height	800	1000	1200
C: Y-axis Way	800	1000	1200
D: U/S 2nd	200	250	300

The formula  $CCD = 2^k + 2k + 6$ , where  $k$  is the number of factors with replications at the design centre, was used to produce the numerical experiment runs. The minimal point was estimated and fitted using a quadratic model for optimisation. The mathematical model for each answer was created using these data points, as indicated in Equation (1).

$$\sigma_{est} = \sqrt{\frac{\sum(Y-Y')^2}{N}} \quad (1)$$

where  $\sigma$  denotes the predicted response,  $Y$  are the input variables, and  $N$  is the interaction coefficient.

## 5. DISCUSSION AND RESULTS

### 5.1 Regression Model and Analysis of Variance (ANOVA) for Wire Bond Strength

Based on the highest-order polynomials recommended by the Design – Expert 13 software (Stat-Ease, Inc., Minneapolis, MN, USA), the regression models for the answers were chosen. For optimising the parameters for Au-Al wire bond system, a quadratic model was used because it provided the best fit. Since a 95% confidence level was chosen for the study, the p-value of the model, which is derived from ANOVA, cannot be more than 0.05. The final empirical models are given in terms of actual factors A, B, C, and D (cf. Table 4) for the wire bond strength of Au-Al bonding system:

$$\text{Wire bond strength} = +52.92518 - 0.113611A - 0.006528B + 0.054664C - 0.468844D + 0.000050AB + 0.000250AD - 6.25 \times 10^{-6}BC - 0.000024C^2 + 0.000819D^2 \quad (2)$$



**Table 4** Proposed solution report for the optimisation process of wire bond strength in Au-Al wire bond system

Source	Sum of Squares	df	Mean Square	F-Value	P-value	PC%	
<b>Model</b>	28.82	9	3.20	14.62	<0.00001		significant
<b>A (Time 1<sup>st</sup>)</b>	0.055	1	0.56	0.25	0.62	0.16	
<b>B (Loop Height)</b>	0.055	1	0.56	0.25	0.62	0.16	
<b>C (Y-axis way)</b>	0.50	1	0.50	2.28	0.15	1.46	
<b>D (U/S 2<sup>nd</sup>)</b>	0.50	1	0.50	2.28	0.15	1.46	
<b>AB</b>	4.00	1	4.00	18.26	0.00004	11.66	
<b>AD</b>	6.25	1	6.25	28.53	<0.00001	18.22	
<b>BC</b>	1.00	1	1.00	4.57	0.045	2.91	
<b>C<sup>2</sup></b>	3.12	1	3.12	14.24	0.0012	9.09	
<b>D<sup>2</sup></b>	14.45	1	14.45	65.98	<0.0001	42.11	
<b>Residual</b>	4.38	20	0.22			12.77	
<b>Lack of Fit</b>	4.38	15	0.30				
<b>Pure Error</b>	0.00	5	0.00				
<b>Cor Total</b>	34.41	29					
<b>Std. Dev.</b>	0.46		<b>R<sup>2</sup></b>		0.868047		
<b>Mean</b>	5.40		<b>Adjusted R<sup>2</sup></b>		0.808669		
<b>C.V. %</b>	8.67		<b>Predicted R<sup>2</sup></b>		0.671161		
			<b>Adeq. Precision</b>		13.69734		

In this statistical analysis, the coefficient of determination ( $R^2$ ), a statistical metric used to evaluate the goodness of fit of the regression line to the actual data points, is the focus of interest. A higher  $R^2$  value indicates a better predictive performance of the model regarding the system. The information from ANOVA indicates that  $R^2$  is 0.868047, proving that the chosen quadratic models are good response predictors. Furthermore, the values (p-value) are less than 0.05, which indicates that the designed model is significant. It should be emphasized that the pure error was recorded as zero because the repeated runs produced the least amount of error possible for the experimental job. The experimental results were accurately distributed around the mean value, as seen by the low coefficient of variation (C.V.) value.

Table 4 indicates that the y-axis way (C) (percentage contribution (PC): 1.46%) and ultrasonic at the second bonding site (D) (PC: 1.46%) has a greater effect on bonding quality compared to time on the first bonding site (A) (PC: 0.16%) and loop height (B) (PC:0.16%). However, the combination of interactions between the parameters contributes better than a single parameter. From Table 4, it is shown that the percentage contribution of interaction between Time 1<sup>st</sup> (A) and U/S 2<sup>nd</sup> (D) is stronger at (PC: 18.22%) compared to only the highest PC of 1.46% from a single parameter.

Figure 7 plots the projected central composite design for Au-Al wire bond system results against the actual results.

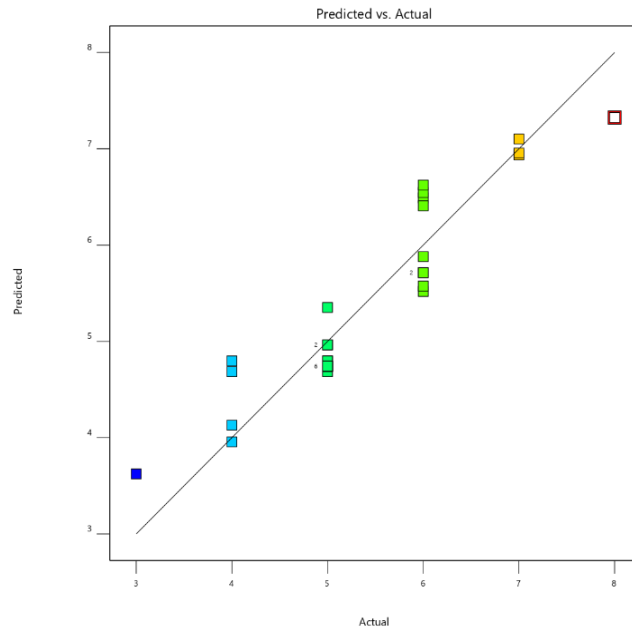


**Figure 7.** Projected central composite design for wire bond strength against the actual results

The graph in Figure 7 aids in identifying values that the regression model has difficulty predicting. The plots show that each model offers a strong fit, and as a result, the created model's projected and obtained values coincide with the actual experimental findings. It is clearly visible from the graph that most of the values of the wire bond strength fall in the proximity of the centreline, which indicates the model is fitted in better terms. The actual and predicted models were the important parts that determined the wire bond strength in the Au-Al wire bond system.

The residuals vs projected wire bond strength for the Au-Al wire bond system are displayed in Figure 8.

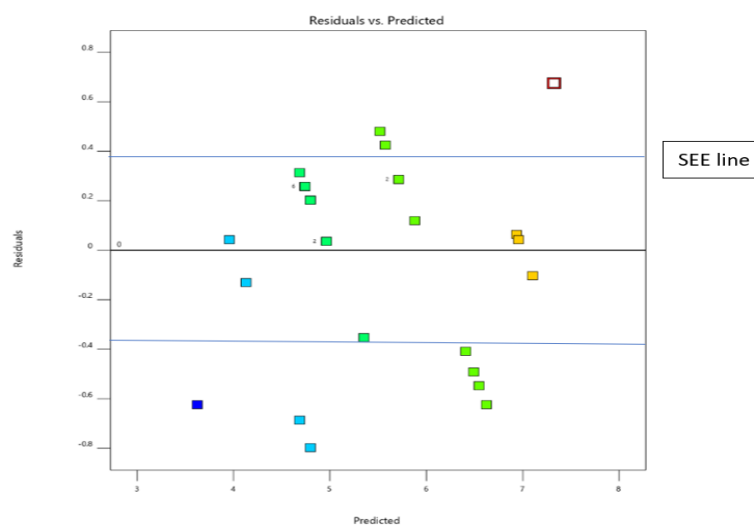


**Figure 8.** Wire bond strength analysis for residuals and predicted plot.

It denotes that the variance of the original observation acquired remains constant for all values of the answer in terms of the scatter plot, indicating that there is no need to modify the response variables. Since two-thirds of the data points fall within the standard error estimation (SEE), which is above or below the least squares line for a data set with a normal linear relationship, the RSM model is significant and can be used to predict the response [25]. According to Figure 8, the SEE values of wire bond strength for Au and Al are  $\pm 0.38$ . Then for example, if the predicted value of the wire bond test is 5 grams, the actual value is in the range from 4.62 to 5.38 grams.

## 5.2 Effect of Geometry Parameters on Wire Bond Strength

As shown in Figure 9, the perturbation plot was used to determine how sensitive the independent variables (factors) were to the responses of wire bond strength.

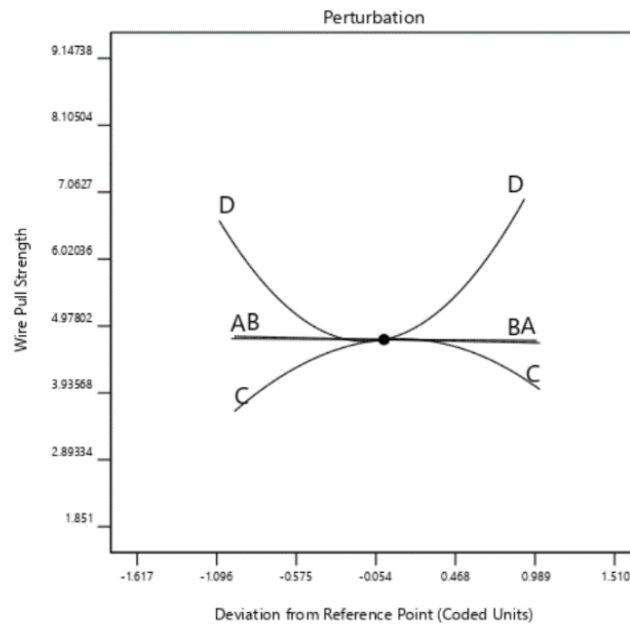


**Figure 9.** Perturbation plot for responses of wire bond strength of Time 1<sup>st</sup> (A), Loop height (B), Y-way (C), U/S 2<sup>nd</sup> (D).

The perturbation plot was utilised to examine the sensitivity of the independent variables (factors) to the responses to wire bond strength, as presented in Figure 9. It is apparent that the wire bond strength for the Au-Al wire bond system is affected by the ultrasonic force at the second bonding site (D) during the wire bonding process. The slope of D decreases from the parameter of 200mN (lower level -1) when it reaches to parameter of 250mN (coded level 0), but the wire bond strength increases when it is at the parameter of 300mN (higher level +1), indicating that ultrasonic force at second bonding improves the wire bond strength, the higher the parameter value. For the bond wire's length from site one to site two (C), the highest value for the wire bond strength was when it was at the lowest parameter of 800mm (coded level 0), indicating that the shorter the distance of wire bond from site one to site two, the higher the wire bond strength. Time on the first bonding site (A) and the height of the wire looping (B), shows a modest influence on the wire bond strength in this study since its variation from lower level -1 to higher level +1 results in insignificant changes in wire bond strength.

Based on the 3D response surface, it was possible to determine the interacting relationship between two of the most important components. In this instance, the decision is made based on the perturbation plots' depicted level of significance to the responses. In Figure 10, shows the contour plots and 3D response surfaces of the quadratic and linear models for the Au-Al wire bond system for Time 1<sup>st</sup> and U/S 2<sup>nd</sup>.

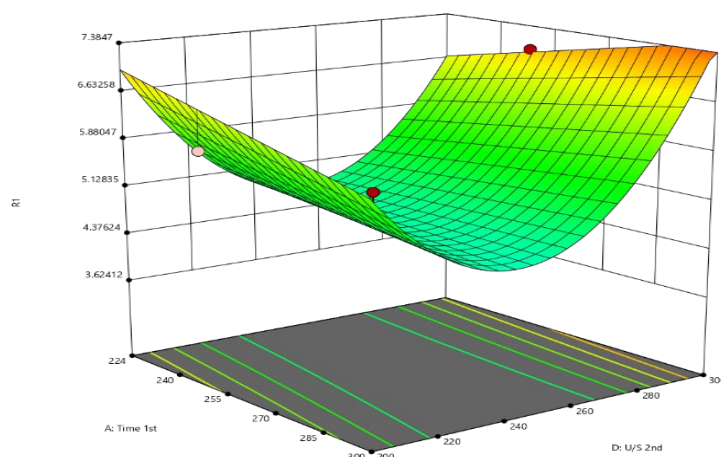


**Figure 10.** 3D responses surface for Time and U/S 2<sup>nd</sup> shows how the two parameters influences the wire bond strength analysis.

In Figure 10, one of the interactions that influence the wire bond strength is the combination of time ultrasonic force at the second bonding (D) and time on the first bonding site (A). It is shown, the highest wire bond strength is identified at parameter 300mN for U/S 2<sup>nd</sup> and parameter 300ms for Time 1st. Both two parameters' interactions contributed to the highest wire bond strength value compared with other interactions recorded in this study. From this, the higher the parameter value of ultrasonic force at the second bonding site (300mN) and the longer the time of bonding on the first bonding site (300ms), the higher the value of wire bond strength, thus, increasing the quality of wire bond in Au-Al system. The relationship between ultrasonic force and time of bonding in wire bonding is a critical aspect of the wire bonding process. This relationship can impact the quality and reliability of the wire bond connections. The ultrasonic force applied during bonding is responsible for creating the necessary mechanical contact and deformation of the wire and bonding pads. Bond strength is often directly related to the ultrasonic force. Higher force levels can result in stronger bonds. The time of bonding, on the other hand, influences how long the bond interfaces are subjected to ultrasonic energy, which affects the quality of the bond formation [26-27]. Hence, any value inserted into these parameters will dictate the wire bond strength analysis.

In Figure 11, shows the contour plots and 3D response surfaces of the quadratic and linear models for the Au-Al wire bond system for Loop Height and Y-axis way.

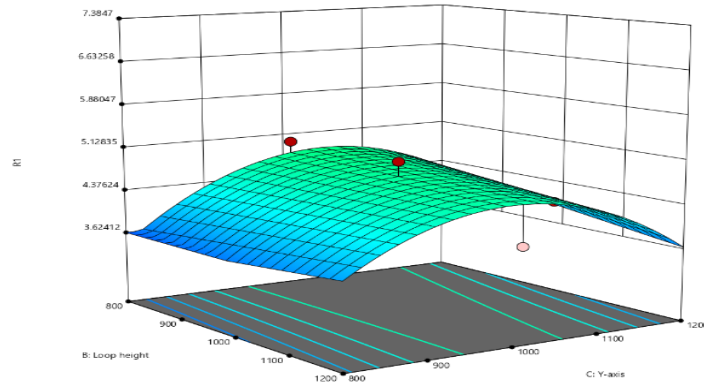


**Figure 11.** 3D responses surface for Loop height and Y-axis shows how the two parameters affect wire bond strength analysis.

In Figure 11, the interaction that influences the wire bond strength in the model is the bond wire's length from site one to site two (B) and the height of the wire looping (C). Depicted from the figure, the peak wire bond strength is recorded at parameter 1000mm for the Y-axis way and 1000mm for loop height. Both two parameters' interactions contributed to the lowest wire bond strength value compared with other interactions recorded in this experiment. The relationship between the wire length between bonding sites (span length) and the height of looping in a wire bond is an important consideration in wire bonding processes, particularly for controlling the quality and reliability of the bonds. Controlling the span length in wire bonding is important due to several issues. Excessive span length can lead to wire sagging, contact problems, and potential damage to the connecting wire, furthermore, insufficient span length would make the connecting wire tighter, possibly damaging the wire. In a similar manner, excessive looping height results in the wire sagging, insufficient looping height causes the wire to be more tense [28-2]. Therefore, the goal is to strike a balance between having enough tension by controlling the span length and the looping height without applying excessive or insufficient force that could damage the connecting wire and the bonding pads. Based on Figure 11, this is the reason why the highest wire bond strength is recorded at the middle ranges for interaction between the wire's length from bond site one to two and looping height.

In Figure 12, shows the contour plots and 3D response surfaces of the quadratic and linear models for the Au-Al wire bond system for Time and Loop Height.

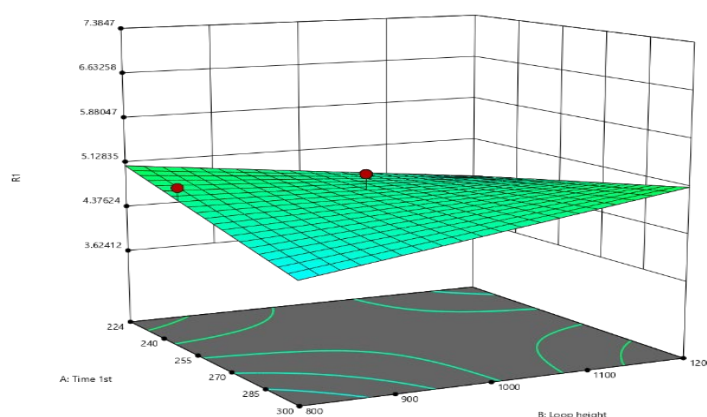


**Figure 12.** 3D responses surface for Time and Loop Height shows how these two parameters affects wire bond strength analysis.

In Figure 12, the interaction that impacts the wire bond strength in the model is Time 1<sup>st</sup> (A) and loop height (B). It is revealed that the highest wire bond strength is gathered at parameter 200ms for Time 1<sup>st</sup> and 800mm for loop height and the second peak pull strength was at 300ms for Time 1<sup>st</sup> (A) and 1200mm for loop height (B). The interactions of these two variables contributed to the second-highest wire bond strength in this study. In wire bonding, the correlation between time of bonding and loop height is an important consideration in achieving optimal wire bonding results. Increasing the bonding time typically results in higher loop height. When extending the duration of the time bond, the wire has more time to form a larger loop before the bonding tool moves away from the bonding pad. A higher loop height can be beneficial such as to enhance the mechanical robustness of the wire bond but there is a limit to how high the loop can be before it becomes problematic. Reducing the bonding time generally leads to lower loop height. A shorter bonding time means that the bonding tool moves away from the bonding pad more quickly, resulting in a smaller loop height formation. Lower loop heights are preferred when the application requires precise control [30]. Thus, the choice of bonding time and loop height should be based on the specific requirements of the semiconductor or microelectronics application.

### 5.3 Optimization Result of Wire Bond Strength in Au-Al Wire Bond System

System optimization was conducted to optimise the responses with the optimal factor setting. Each factor's desired outcome was set to "in range". Using the Design-Expert 13 software, a total of 100 solutions were discovered. These solutions depend on how well the goal criteria are achieved and expressed in desirability. Higher desirability is desired in optimization as it indicates nearness to the targeted goal criteria. In this study, the highest desirability of 0.994 was obtained, while the lowest desirability was 0.805.

The ramp plot for the optimized system using the desirability function is depicted in Figure 13. The wire bond strength was recorded as the highest when the factors were set at: Time at first bonding site (Time 1<sup>st</sup>) at 300ms, wire looping height (loop height) at 1200mm, wire bond Y-axis length at 992mm, and ultrasonic force at second bonding site (U/S 2<sup>nd</sup>) at 300mN.

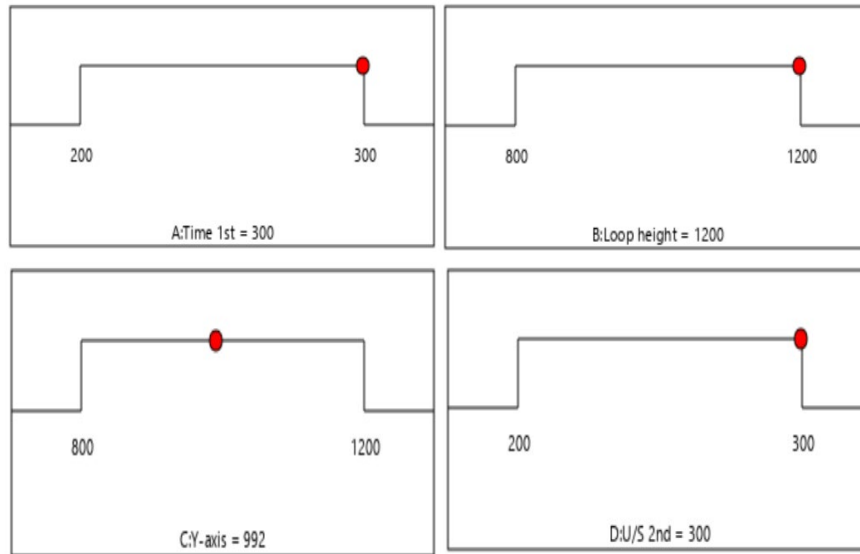


**Figure 13.** Ramp plot of system optimization.

#### 5.4 Validation Test

The Design-Expert 13 software's point prediction capability was used to predict the bonding time at the first bonding site (Time 1<sup>st</sup>), the height of the wire looping (Loop height), the length of the bond wire between sites one and two (Y-way), and the ultrasonic force at site two (U/S 2<sup>nd</sup>) of the chosen experiments. The prediction interval was 95%. Table 5 below displays the experimental and expected data. Notably, the wire bond strength percentage errors between the predicted and experimental data were calculated as 0.91% to 7.05%.

The empirical models created for the study are capable of being considered reasonably accurate. The confirmation run's actual numbers fell inside the 95% prediction interval, which is the range that was anticipated at any given value to fall into 95% of the time.

**Table 5** Predicted, actual, and percentage error data

Time 1 <sup>st</sup> (ms)	Loop Height	Y-way	U/S 2 <sup>nd</sup>	Predicted	Actual	Residual	Error (%)
300	1000	1000	250	4.68	5	-0.31	6.27
300	1200	1200	200	5.35	5	0.35	7.05
300	1200	1200	300	6.93	7	-0.064	0.91

#### 6. CONCLUSION

This paper presents a solution for performing wire bonding in an Au-Al system with the most optimised parameters involved, to improve the quality of the wire bonding and reduce the manufacturing defects that might occur in this system. Statistical analysis was used to identify significant parameters and suggest a preferable wire bonding equipment with the objective of investigating the most optimised set of parameters to be used in Au-Al wire bond system. In the validation test, the Au-Al wire bond system was modeled and experimentally confirmed with the effectiveness of the proposed sets of parameters. This model can be used to predict the value of wire bond test value when using the Au-Al wire bonding system.

Engineers will be able to predict the outcome of the wire bond test value and the quality of wire bonding, to ensure compliance with customer requirements in this industry. The major experimental findings are summarised as follows:

1. It is shown that the combination of interactions between the parameters contributes better PC (percentage contribution) than a single parameter. The highest percentage contribution from a single parameter was ultrasonic at the second bonding site (PC: 1.46%), meanwhile, the highest percentage contribution for the combination of interactions of parameters was time of bond at 1<sup>st</sup> bond site and ultrasonic force at 2<sup>nd</sup> bond site (PC: 18.22%).
2. To predict the values of the outcomes within the parameters of the components examined, regression models for the responses were created. The  $R^2$  for all replies is above 80% in terms of a good fit model, indicating that the regression models are significant and may be utilised for predicting the ideal configuration. Additionally, there is a difference between the predicted and adjusted  $R^2$  of less than 0.2, which is in reasonable agreement.
3. Optimisation of Au-Al wire bond system, the optimum value for parameters in performing Au-Al wire bond system was proposed. Based on the goal, constraint, and wire bond test value, one solution with its desirability in index levels of 0.994 was proposed. The combination of Time 1<sup>st</sup> selected for 300, Loop height selected for 1200 Y-axis selected for 996, and U/S 2<sup>nd</sup> force selected for 300, in terms of the value of wire bond test, was found to be an optimum value in conducting Au-Al wire bond system, ensuring the highest quality of wire bond.
4. Based on the selected optimized values for the Au-Al wire bonding system, a validation test was conducted to validate the effectiveness of the experimental method. From the validation results, the relative error between the predicted and actual value was calculated to be at 6.27%, 7.05%, and 0.91% confirming the proposed optimization.
5. Au-Al wire bonding is a commonly used technique in the semiconductor and microelectronics industry but it has several limitations. Au-Al bonds have lower bond strength compared to pure Au bonds. This resulted in many bond failures during this research. Also, the aluminium from this system can diffuse into the semiconductor material, potentially causing reliability problems, if high-temperature environments were introduced. Thus, to address these limitations for future research, one of the ways is to optimize bonding parameters such as bonding force, time of bond, looping height, span length, and ultrasonic force to improve the strength and reliability of the bond. The other is to use barrier layers or coatings on the aluminium substrate to prevent aluminium diffusion into the semiconductor material.

## ACKNOWLEDGEMENTS

The authors gratefully acknowledge the Ministry of Higher Education Malaysia for supporting this research through the Fundamental Research Grant Scheme (Project Code: FRGS/1/2021/TK0/USM/03/9). Additionally, the authors extend their appreciation to Universiti Sains Malaysia and Department of Microelectronic Technologies, Advanced Technology Training Centre for their invaluable technical assistance.



## REFERENCES

- [1] H.-K. Kung, B.-W. Huang, and H.-C. Hsu. "The Effect of Cross-Section Geometry of Bonding Wire on Wire Sweep for Semiconductor Packages," (2017).
- [2] M. A. Alim, M. Z. Abdullah, M. S. A. Aziz, and R. Kamarudin. "Die attachment, wire bonding, and encapsulation process in LED packaging: A review," *Sensors and Actuators, A: Physical*, vol. 329. Elsevier B.V., (2021), doi: 10.1016/j.sna.2021.112817.
- [3] H. Xu, C. Liu, V. V. Silberschmidt, Z. Chen, and J. Wei, "The role of bonding duration in wire bond formation: A study of footprints of thermosonic gold wire on aluminium pad," *Microelectronics International*, vol. 27, no. 1, (2010), pp. 11–16, doi: 10.1108/13565361011009469.
- [4] R. Lyn and W. Crockett. "SEMICON ® Singapore 2007 Assembly Using X-Wire™ Insulated Bonding Wire Technology." (2007).
- [5] A. C. Fischer, J. G. Korvink, N. Roxhed, G. Stemme, U. Wallrabe, and F. Niklaus "Unconventional applications of wire bonding create opportunities for microsystem integration," *Journal of Micromechanics and Microengineering*, vol. 23. (2013) doi: 10.1088/0960-1317/23/8/083001.
- [6] H. Zhou *et al.* "Research Progress on Bonding Wire for Microelectronic Packaging," *Micromachines*, vol. 14, no. 2. (2023). MDP. doi: 10.3390/mi14020432.
- [7] A. Shah, M. Mayer, Y. Zhou, S. J. Hong, and J. T. Moon. "In situ ultrasonic force signals during low-temperature thermosonic copper wire bonding," *Microelectron Eng*, vol. 85, no. 9, (2008) pp. 1851–1857, doi: 10.1016/j.mee.2008.05.035.
- [8] Ana Sofia Ramos, "Intermetallics," *Metals*, vol. 7, no. 10. MDPI AG, Coimbra, Portugal, (2017). doi: 10.3390/met7100446.
- [9] Denis V. Vertyanov, Igor A. Belyakov, and Sergey P. Timoshenkov, "Effects of Gold-aluminium Intermetallic Compounds on Chip Wire Bonding Interconnections Reliability". (2020), IEEE.
- [10] M. J. Mccracken, "Assessing Au-Al Wire Bond Reliability Using Integrated Stress Sensors," (2010).
- [11] S. Murali, N. Srikanth, and C. J. Vath, "Effect of wire size on the formation of intermetallics and Kirkendall voids on thermal aging of thermosonic wire bonds," *Mater Lett*, vol. 58, no. 25, pp. 3096–3101, (Oct. 2004), doi: 10.1016/j.matlet.2004.05.070.
- [12] Z. W. Zhong. "Overview of wire bonding using copper wire or insulated wire," *Microelectronics Reliability*, vol. 51, no. 1, pp. 4–12, (Jan. 2011), doi: 10.1016/j.microrel.2010.06.003.
- [13] P. S. Chauhan, A. Choubey, Z. Zhong, and M. G. Pecht. "Copper wire bonding", vol. 9781461457619. Springer New York. doi: 10.1007/978-1-4614-5761-9, (2014)
- [14] C. E. Tan, "Low Cost & High-Quality Copper Wire Bonding in Increasing Market Growth," (2014).
- [15] C. D. Breach, "The great debate: Copper vs. gold ball bonding What is the future of bonding wire? Will copper entirely replace gold? (2019)." [Online]. Available: [www.goldbulletin.org](http://www.goldbulletin.org).
- [16] C. R. Morgan, A. Russell, and G. Tuttle, "Investigation of gold-aluminium intermetallic formations and their degradation mechanisms in Ball Grid Array (BGA) Multi Chip Modules (MCM)," (2004).
- [17] Vesa Vuorinen, Markus Turunen, and Toni Mattila, "Interfacial Compatibility in Microelectronics: Moving Away from the Trial-and-Error Approach," (2012). [Online]. Available: <http://www.springer.com/series/6289>.
- [18] H. Xu, V.L. Acoff, and C. Liu (2011). *Void Growth in Thermosonic Copper/Gold Wire Bonding on Aluminium Pads*.
- [19] J. Beleran, F. Wulff, and C. D. Breach, "Gold ball-bond mechanical reliability at 40pm pitch: squash height and bake temperature effects.," (2004).
- [20] I. Singh, S. Assembly Packaging Engineer, J. Brumer, S. Process Eng, and A. Packaging (2003). "Reliability Ground Rules Change at <50 pm Pitch."

- [21] K. Tamala, P. Engineer, and O. Kwon. "SEMICON @ Singapore 2006 Resolution of a Fine Pitch Wire Bonding Reliability Problem," (2006).
- [22] T. Matsumae, Y. Kurashima, H. Umezawa, Y. Mokuno, and H. Takagi, "Room-temperature bonding of single-crystal diamond and Si using Au/Au atomic diffusion bonding in atmospheric air," *Microelectron Eng*, vol. 195, (2018) pp. 68–73, doi: 10.1016/j.mee.2018.03.025.
- [23] A. Tony *et al.*, "A Preliminary Experimental Study of Polydimethylsiloxane (PDMS)-To-PDMS Bonding Using Oxygen Plasma Treatment Incorporating Isopropyl Alcohol," *Polymers (Basel)*, vol. 15, no. 4, (2023), doi: 10.3390/polym15041006.
- [24] S. K. Behera, H. Meena, S. Chakraborty, and B. C. Meikap, "Application of response surface methodology (RSM) for optimization of leaching parameters for ash reduction from low-grade coal," *Int J Min Sci Technol*, vol. 28, no. 4, (2018) pp. 621–629, doi: 10.1016/j.ijmst.2018.04.014.
- [25] V. Bewick, L. Cheek, and J. Ball, "Statistics review 7: Correlation and regression," *Critical Care*, vol. 7, no. 6, (2003) pp. 451–459, doi: 10.1186/cc2401.
- [26] M. D. McKay, "Scholar Commons the Effect of Ultrasonic Power in Aluminium Wire Bonding Hardness Profiles Recommended Citation," (2018). Available: [https://scholarcommons.scu.edu/cgi/viewcontent.cgi?article=1035&context=mech\\_mstr](https://scholarcommons.scu.edu/cgi/viewcontent.cgi?article=1035&context=mech_mstr).
- [27] K. S. Goh and Z. W. Zhong, "Development of capillaries for wire bonding of low-k ultra-fine-pitch devices," *Microelectron Eng*, vol. 83, no. 10, (2006). pp. 2009–2014, , doi: 10.1016/j.mee.2006.04.003.
- [28] Reid, P., "Optimizing the wire bond process collaboration is the key,". (2007). pp.40-44.
- [29] D. S. Liu, Y. C. Chao, and C. H. Wang, "Study of wire bonding looping formation in the electronic packaging process using the three-dimensional finite element method," *Finite Elements in Analysis and Design*, vol. 40, no. 3, pp. 263–286, (Jan. 2004), doi: 10.1016/S0168-874X(02)00226-3.
- [30] F. Wang and Y. Chen, "Experimental and modelling studies of looping process for wire bonding," *Journal of Electronic Packaging, Transactions of the ASME*, vol. 135, no. 4, pp. 41009-1-41009–9, (2013), doi: 10.1115/1.4025667.